2-2015

Tunable Narrow Band Difference Frequency THz Wave Generation in DAST via Dual Seed PPLN OPG

Brian Dolasinski
University of Dayton, dolasinskib1@udayton.edu

Peter E. Powers
University of Dayton

Joseph W. Haus
University of Dayton, jhaus1@udayton.edu

Adam Cooney
Air Force Research Laboratory

Tunable narrow band difference frequency THz wave generation in DAST via dual seed PPLN OPG

Brian Dolasinski,[1*] Peter E. Powers,[1, 2] Joseph W. Haus,[1] and Adam Cooney[3]

[1]*Electro-Optics Program, University of Dayton, 300 College Park, Dayton, Ohio 45469, USA*
[2]*Physics Department, University of Dayton, 300 College Park, Dayton, Ohio 45469, USA*
[3]*Air Force Research Laboratory, Wright Patterson AFB, Ohio 45433, USA*
[*]*dolasinskib1@udayton.edu*

Abstract: We report a widely tunable narrowband terahertz (THz) source via difference frequency generation (DFG). A narrowband THz source uses the output of dual seeded periodically poled lithium niobate (PPLN) optical parametric generators (OPG) combined in the nonlinear crystal 4-dimthylamino-N-methyl-4-stilbazolium-tosylate (DAST). We demonstrate a seamlessly tunable THZ output that tunes from 1.5 THz to 27 THz with a minimum bandwidth of 3.1 GHz. The effects of dispersive phase matching, two-photon absorption, and polarization were examined and compared to a power emission model that consisted of the current accepted parameters of DAST.

OCIS codes: (190.0190) Nonlinear optics; (190.4400) Nonlinear optics, materials.

Reference and Links

1. T. Taniuchi, S. Okada, and H. Nakanishi, "Widely tunable terahertz-wave generation in an organic crystal and its spectroscopic application," J. Appl. Phys. **95**(11), 5984–5988 (2004).
2. P. E. Powers, R. A. Alkuwari, J. W. Haus, K. Suizu, and H. Ito, "Terahertz generation with tandem seeded optical parametric generators," Opt. Lett. **30**(6), 640–642 (2005).
3. B. Monoszlai, C. Vicario, M. Jazbinsek, and C. P. Hauri, "High-energy terahertz pulses from organic crystals: DAST and DSTMS pumped at Ti:sapphire wavelength," Opt. Lett. **38**(23), 5106–5109 (2013).
4. D. H. Jundt, "Temperature-dependent Sellmeier equation for the index of refraction, n_e, in congruent lithium niobate," Opt. Lett. **22**(20), 1553–1555 (1997).
5. K. Suizu, K. Miyamoto, T. Yamashita, and H. Ito, "High-power terahertz-wave generation using DAST crystal and detection using mid-infrared powermeter," Opt. Lett. **32**(19), 2885–2887 (2007).
6. D. Xu, P. Liu, Y. Wang, K. Zhong, W. Shi, and J. Yao, "Monochromatic tunable terahertz source base on nonlinear optics," J. Elect. Sci. Tech. **11**(4), 339–348 (2008).
7. G. Knopfle, R. Schlesser, R. Ducret, and P. Gunter, "Optical and nonlinear optical properties of 4'-dimethylamino-N-methyl-stilbazolium tosylate (DAST) crystals," Nonlinear Opt **9**, 143 (1995).
8. P. Y. Han, M. Tani, F. Pan, and X. C. Zhang, "Use of the organic crystal DAST for terahertz beam applications," Opt. Lett. **25**(9), 675–677 (2000).
9. P. Zhao, B. Zhang, E. Li, R. Zhou, D. Xu, Y. Lu, T. Zhang, F. Ji, X. Zhu, P. Wang, and J. Yao, "Experimental study on a high conversion efficiency, low threshold, high-repetition-rate periodically poled lithium niobate optical parametric generator," Opt. Express **14**(16), 7224–7229 (2006).
10. M. Jazbinsek, L. Mutter, and P. Gunter, "Photonic applications with the organic nonlinear optical crystal DAST," IEEE J. Quantum Electron. **14**(5), 1298–1311 (2008).
11. S. Russell, M. J. Missey, P. Powers, and K. Schepler,S. Brueck, R. Fields, M. Fejer, and F. Leonberger, eds., "Periodically poled lithium niobate with a 20° fan angle for continuous OPG tuning," in *Conference on Lasers and Electro-Optics*, S. Brueck, R. Fields, M. Fejer, and F. Leonberger, eds., OSA Technical Digest (Optical Society of America, 2000), paper CFN6.
12. K. Kawase, M. Mizuno, S. Sohma, H. Takahashi, T. Taniuchi, Y. Urata, S. Wada, H. Tashiro, and H. Ito, "Difference-frequency terahertz-wave generation from 4-dimethylamino-N-methyl-4-stilbazolium-tosylate by use of an electronically tuned Ti:sapphire laser," Opt. Lett. **24**(15), 1065–1067 (1999).
13. S. Ohno, K. Miyamoto, H. Minamide, and H. Ito, "New method to determine the refractive index and the absorption coefficient of organic nonlinear crystals in the ultra-wideband THz region," Opt. Express **18**(16), 17306–17312 (2010).

#229102 - $15.00 USD Received 4 Dec 2014; revised 18 Jan 2015; accepted 20 Jan 2015; published 5 Feb 2015

14. M. Walther, K. Jensby, S. R. Keiding, H. Takahashi, and H. Ito, "Far-infrared properties of DAST," Opt. Lett. **25**(12), 911–913 (2000).
15. K. Nawata, Y. Miyake, S. Hayashi, T. Notake, H. Kawamata, T. Matsukawa, F. Qi, and H. Minamide, "Study of efficient optical parametric generation in KTP crystal as pump source for DAST-DFG," in *CLEO: 2013*, OSA Technical Digest (online) (Optical Society of America, 2013), paper JTh2A.52.
16. E. Hérault, S. Forget, G. Lucas-Leclin, and P. Georges, "Continuously tunable visible compact laser source using optical parametric generation in microlaser-pumped periodically poled lithium niobate," in *Advanced Solid-State Photonics*, J. Zayhowski, ed., Vol. 83 of OSA Trends in Optics and Photonics (Optical Society of America, 2003), paper 339.
17. L. S. Rothman, C. P. Rinsland, A. Goldman, S. T. Massie, D. P. Edwards, J. M. Flaud, A. Perrin, C. Camy-Peyret, V. Dana, J. Y. Mandin, J. Schroeder, A. McCann, R. R. Gamache, R. B. Wattson, K. Yoshino, K. V. Chance, K. W. Jucks, L. R. Brown, V. Nemtchinov, and P. Varanasi, "The HITRAN molecular spectroscopic database and HAWKS (HITRAN atmospheric workstation) 1996 edition," J. Quant. Spectrosc. Radiat. Transf. **60**(5), 665–710 (1998).
18. T. Notake, K. Nawata, H. Kawamata, T. Matsukawa, F. Qi, and H. Minamide, "Development of an ultra-widely tunable DFG-THz source with switching between organic nonlinear crystals pumped with a dual-wavelength BBO optical parametric oscillator," Opt. Express **20**(23), 25850–25857 (2012).

1. Introduction

Terahertz (THz) wave radiation, also called sub-millimeter waves or T-waves, can be harnessed for applications to imaging, sensing and molecular spectroscopy. Its unique position in the electromagnetic spectrum covering a range from about 0.3 THz to 30 THz make it a subject of studies exploring uses in fields of security, medicine and nondestructive inspection. In the pursuit of developing new THz technology several schemes are available to generate and detect THz radiation. THz research has been a fruitful field for both theoretical and experimental explorations [1].

In many studies, broad-bandwidth mode locked femtosecond lasers with high peak power pulses have been utilized with nonlinear crystals to generate broadband THz radiation. Other promising schemes for the generation of high power, narrow-band, sub-millimeter waves employs nonlinear difference frequency generation (DFG) between two laser sources combined in a crystal with a high nonlinear coefficient. Generation of widely tunable THz radiation sources have used nonlinear optical parametric oscillation (OPO) [1], and optical parametric generation (OPG) [2]. Multiple advantages are associated with the DFG method that facilitate wide band tunability with narrow bandwidth THz waves. However, multiple limitations are present when the DFG process is employed with OPO configurations. The methods that involve OPO schemes result in drawbacks such as mode hopping and broad bandwidth [3]. The aforementioned drawbacks limit the OPO-DFG schemes to few applications. The THz region is an attractive avenue for the development of technology that encompass applications in nondestructive evaluation such as standoff detection, and packaging inspection imaging. Many of the applications require that such a system possess the inherent ability for wide tunability with a narrow bandwidth to optimize the object transparency or material fingerprint. In this paper we present a method that consists of dual tunable OPGs to generate narrow bandwidth to serve as DFG mixing frequencies for the emission of THz waves over a broad spectrum.

We report continuous THz generation with an emission spectrum of 1.5 THz to 27 THz operating with seamless tunability and a minimum bandwidth of 3.1 GHz. The main advantage of using the OPG method is simplicity. The method only requires that a pump source be co-aligned with a tunable diode laser injection seed for a single pass through the nonlinear OPG crystal. Thus, the process obviates the necessity of using a resonator cavity. The configuration facilitates the ease of adjustment to the system and the rejection of coatings that are necessary for tunable OPO systems operating at high power. With the removal of the aforementioned cavity the insertion of an injection seeder can be accomplished with ease. In this configuration, the pump source is co-aligned with a single seed source in which a fraction of the pump beam is frequency converted into a narrow linewidth signal and idler pair. Magnesium oxide (MgO) doped periodically poled lithium niobate (PPLN) crystal was

#229102 - $15.00 USD Received 4 Dec 2014; revised 18 Jan 2015; accepted 20 Jan 2015; published 5 Feb 2015

selected for its inherent high conversion efficiency [4]. Our system is comprised of dual injection seed OPG PPLN stages; their output beams are co-aligned for transmission through a DAST crystal for the DFG of THz wave radiation. The method is based on the theory that the output signal power from the DFG process depends strongly on the index, absorption, and frequency mixing of the co-aligned sources in the nonlinear medium of DAST. In which DAST has significant nonlinear coefficients of d_{111} = 260 pm/V, d_{122} = 40 pm/V, and d_{266} = 39 pm/V [5, 6, 7].

2. Theory

In our DFG method two detuned signal beams are co-aligned and passed through the nonlinear crystal DAST of thickness L. The index of refraction for the crystal in the optical and THz region are very similar [8]. Phase matching can occur with type zero and other polarization combinations with respect to the cut of the crystal which results in the down conversion from the optical regime to THz frequencies. In order to generate the two widely tunable signal beams a single pump frequency is equally divided and passed through two different types of PPLN crystals. In each PPLN crystal the pump frequency is spontaneously converted to a signal and idler pair due to the inherent nonlinearity at the selected index [4]. The generated signal idler pair is a result of quasi-phase matching which is dependent on factors such as crystal temperature, PPLN poling, and pump frequency. QPM was selected over traditional birefringent phase-matching (BPM) because the output beams are naturally co-aligned. QPM periodically re-orientates regions of the lithium niobate crystal in order to reset the phase of the nonlinear polarization and maintain a coherent buildup of the signal and idler wave conversion. QPM with high conversion efficiency can be maintained over a large spectral range [9]. The functional form of QPM in this process is given by

$$\Delta k = k_p - k_s - k_i - \frac{2\pi}{\Lambda} = 2\pi\left(\frac{n_e(\lambda_p,T)}{\lambda_p} - \frac{n_e(\lambda_s,T)}{\lambda_s} - \frac{n_e(\lambda_i,T)}{\lambda_i} - \frac{1}{\Lambda}\right), \qquad (1)$$

where Λ is the grating periodicity [10]. The extraordinary refractive indices for each wavelength at a given polarization angle Θ and temperature T is $n_e(\lambda_p, T)$, $n_e(\lambda_s, T)$, and $n_e(\lambda_i, T)$.

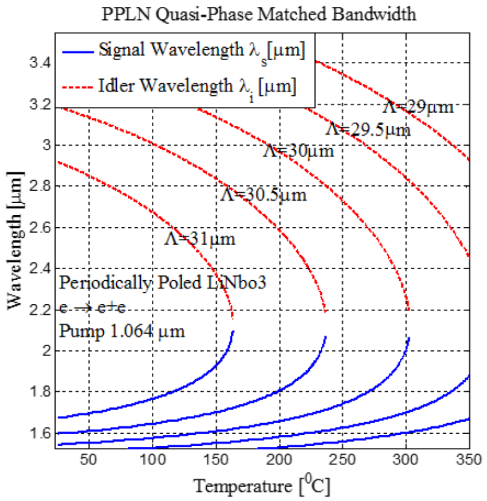

Fig. 1. Multi-grating QPM temperature tuned signal and idler range for PPLN.

#229102 - $15.00 USD Received 4 Dec 2014; revised 18 Jan 2015; accepted 20 Jan 2015; published 5 Feb 2015

Here, we consider the case for two independent PPLN crystal-grating patterns. The first PPLN type is that of a multi-grating periodicity. Due to the spectral range constraints of the available injection diode seeding lasers and our Nd:YAG laser pump laser, the selected grating period spanned the range from about 27 to 31 μm. Thus, OPG wavelength tuning in the multi-grating would be a result of grating period and temperature tuning. The QPM model of the available multi-grating is given in Fig. 1.

Thus, properly chosen multi-grating PPLN samples permit the correct phase matching parameters necessary for injection seeding. However, certain drawbacks occur if both OPG stages were to implement a crystal with only several grating periods; both signal wavelengths would be constrained by the availability of a few grating periods and require large temperature changes. This approach would prevent continuous narrowband tunability. In order to achieve seamless tunability a PPLN crystal with a continuous grating periodicity (fan out) was used [11]. Thus, a single temperature was selected and the crystal was translated to achieve wavelength tunability. The QPM results for the fan out grating period versus signal wavelength is given in Fig. 2.

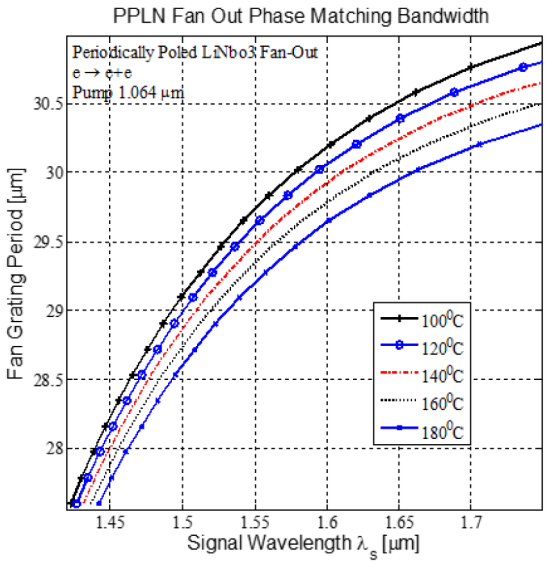

Fig. 2. Fan out grating period and quasi-phase matched signal range for PPLN with temperature tuning variations.

When the two OPG signal wavelengths λ_{s1} and λ_{s2} are co-aligned and incident on the DAST crystal, a THz wavelength λ_{THz} dependent on the wavelength separation is generated. The modeled DFG output power as a function of frequency and polarization angle, in the non-depleted pump and signal limit is written as [12]

$$P_{THz} = Se^{-\alpha_{THz}L}(\eta), \tag{2}$$

$$S = 32\left(\frac{\mu_0}{\varepsilon_0}\right)^{\frac{1}{2}}\left(\frac{2\omega_{THz}d_{eff}L}{(n_e(\lambda_{s1},\theta)+1)(n_e(\lambda_{s2},\theta)+1)(n_e(\lambda_{THz},\theta)+1)}\right)^2\left(\frac{1}{c^2}\right)\left(\frac{P_{\omega_{s1}}P_{\omega_{s2}}}{A}\right), \tag{3}$$

$$\eta = \left(\frac{1+e^{(-\Delta\alpha L)}-2e^{\left(-\frac{1}{2}\Delta\alpha L\right)}\cos(\Delta kL)}{(\Delta kL)^2+(\frac{1}{2}\Delta\alpha L)^2}\right), \tag{4}$$

#229102 - $15.00 USD Received 4 Dec 2014; revised 18 Jan 2015; accepted 20 Jan 2015; published 5 Feb 2015

$$\Delta k = k_{s1} - k_{s2} - k_{THz} = 2\pi\left(\frac{n_e(\lambda_{s1},\theta)}{\lambda_{s1}} - \frac{n_e(\lambda_{s2},\theta)}{\lambda_{s2}} - \frac{n_{e_{THz}}(\lambda_{THz},\theta)}{\lambda_{THz}}\right), \tag{5}$$

$$\Delta\alpha = \alpha_1 - \alpha_2 - \alpha_{THz}. \tag{6}$$

In Eq. (4) and (6), the absorption coefficients for the crystal at each wavelength and polarization angle are given as α_1, α_2 and α_{THz} [10, 14]. The parameter d_{eff} is the nonlinear coefficient for DAST of the desired orientation of the linearly polarization of the combined OPA mixing sources, and L is the DAST crystal length. DAST is a monoclinic crystal, which belongs to the point group m. The d coefficient tensor can be written in contracted index form

$$\begin{bmatrix} d_{11} & d_{12} & d_{13} & 0 & d_{15} & 0 \\ 0 & 0 & 0 & d_{24} & 0 & d_{26} \\ d_{31} & d_{32} & d_{33} & 0 & d_{35} & 0 \end{bmatrix}. \tag{7}$$

The matrix for DAST is simplified for incident mixing fields polarized for the extra-ordinary index and only a combination of a and b axes are considered. Thus, the c axis interaction can be neglected. The matrix representing the nonlinear interaction can be written in a tensor format of the polarization

$$P(\omega_{THz} = \omega_{S_1} - \omega_{S_2}) = 2\varepsilon_0 \begin{bmatrix} d_{11} & d_{12} & d_{13} & 0 & d_{15} & 0 \\ 0 & 0 & 0 & d_{24} & 0 & d_{26} \\ d_{31} & d_{32} & d_{33} & 0 & d_{35} & 0 \end{bmatrix} \begin{bmatrix} A_a(\omega_{S_1})A_a^*(\omega_{S_2}) \\ A_b(\omega_{S_1})A_b^*(\omega_{S_2}) \\ 0 \\ 0 \\ 0 \\ A_a(\omega_{S_1})A_b^*(\omega_{S_2}) + A_b(\omega_{S_1})A_a^*(\omega_{S_2}) \end{bmatrix}. \tag{8}$$

The d_{eff} coefficient for the DFG polarization in DAST becomes a function of angle. All fields are $\hat{e}$ polarized (extraordinary), where θ is the angle between the k-vector and the a axis and ρ is the walk off angle

$$A_{S_1=S_2}\hat{e} = A_{S_1=S_2}[-\cos(\theta+\rho)\hat{a} + \sin(\theta+\rho)\hat{b}]. \tag{9}$$

The extraordinary refractive indices for each wavelength are denoted as $n_e(\lambda_{s1},\theta), n_e(\lambda_{s2},\theta),$ and $n_{e_{THz}}(\lambda_{THz},\theta)$ [10, 13] given by

$$\frac{1}{n_e^2(\theta)} = \frac{\cos^2(\theta)}{n_a^2} + \frac{\sin^2(\theta)}{n_b^2}, \tag{10}$$

where the angle, θ, is measured with respect to the a axis in DAST.

In DFG calculations, different types of phase matching processes are generally used. Usually, two sources are mixed in the DFG crystal that are a combination of extraordinary and ordinary waves. However, efficient THz generation by DFG in DAST is possible using co-aligned and co-polarized pumps at specific polarization angles. This occurs because of the large resonance in the refractive index between the mid-IR and the FIR [5]. Using the components of the dispersion and the extraordinary refractive index in the DAST crystal, we calculate the linear phase matching efficiency and power generation as a function of

#229102 - $15.00 USD Received 4 Dec 2014; revised 18 Jan 2015; accepted 20 Jan 2015; published 5 Feb 2015

polarization angle and frequency. The phase matching efficiency, η, is given in Fig. 3; η is defined in Eq. (4) and absorption is neglected in the figure. The figure depicts where the DAST phase matches efficiently and provides experimental guidance on where to expect a strong signal as a function of polarization angle and frequency. In Fig. 3 one of the signal wavelengths was held constant at λ_{S_1} = 1560.8 nm and the other signal wavelength was tuned from λ_{S_2} = 1380 nm to 1559 nm.

The power of the wave at λ_{THz} is estimated from energy conservation for each of the angular frequencies $\omega_{s1} = \omega_{s2} + \omega_{THz}$. Therefore, we estimate the DFG phase matched output power using the known indices and absorption parameters over the desired spectral range. Using the beam propagation method, we studied nonlinear wave equations with three wavelengths coupled to the d_{111} component from the nonlinear tensor of DAST. The beams were linearly polarized in the a-b plane of the DAST crystal as the wave vector angle was rotated [6, 14]. The simulated DFG output power as a function of frequency and polarization is given in Fig. 4.

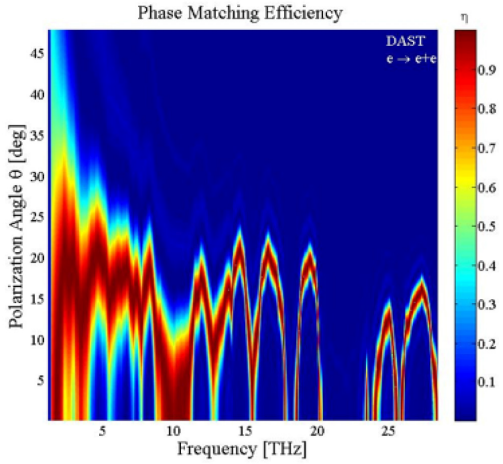

Fig. 3. DAST DFG efficiency, η, versus frequency and polarization angle. η is defined in Eq. (4) and the absorption was neglected. The red color denotes good phase matching regions.

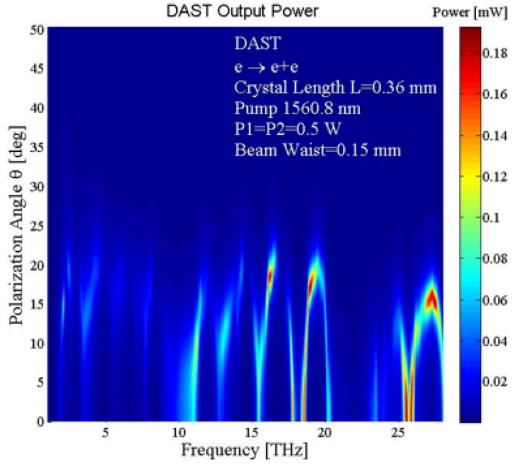

Fig. 4. Power output of DAST DFG as a function of combined OPA polarization angle and difference frequency.

#229102 - $15.00 USD Received 4 Dec 2014; revised 18 Jan 2015; accepted 20 Jan 2015; published 5 Feb 2015

In the model, the signal pump sources were at an average power of 0.5 W, both with the same polarization, and with an identical beam waist of 0.15 mm. Thus, if one were to experimentally implement similar parameters one could theoretically achieve a maximum power of 0.2 mW. It is of note that at lower frequencies at least 0.02 mW is still theoretically achievable. In addition, the DAST crystal should provide a large tuning band of up to 28 THz. Experimentally the linewidth of the generated THz waves should closely follow linewidth of the combined signal waves.

3. System configuration and schematic

A schematic of the experimental configuration is given in Fig. 5. In the diagram, two MgO:PPLN OPG crystals are used in the DFG mixing process. Each crystal is 5 cm long and is 1 mm thick. One MgO:PPLN crystal was grated with a multi-grating pattern. Temperature tuning of the generated spectral range was matched to the seed laser wavelength [16]. The secondary stage was an MgO:PPLN with a fan out grating pattern of 25° which allowed continuous bandwidth tuning by position without temperature tuning. The temperature of the multi-grating PPLN was varied for a variety of wavelengths while fan out crystal was maintained at a temperature of 120°C.

The pump source of each stage was an Nd:YAG of single wavelength at 1.064 μm. The source was Q-switched at 10 kHz with a pulse width of 1 ns. The pump beam was vertically polarized using a half-wave plate with respect to the z-cut MgO:PPLN crystals. The pump source was collimated and equally divided with a beam-splitting cube. Each beam was projected through each MgO:PPLN crystal and focused to a beam waist w of 0.2 mm in the center of the crystals (1/e intensity diameters). The fan out crystal was advanced to maintain an identical path length and phase. Similar performance was measured from each stage. The generated signal wavelength power from each stage was 0.8 W with an average energy per pulse of 80 μJ.

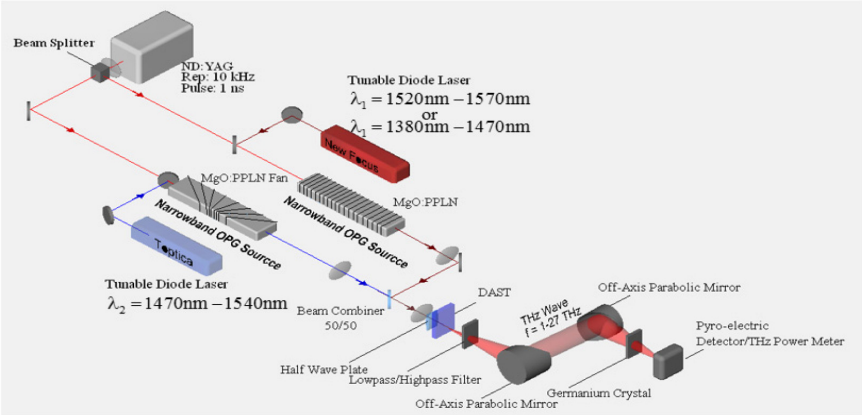

Fig. 5. Experimental setup used to generate a narrowband THz wave. The dual injection seeded OPG is mixed in the DFG crystal DAST.

Diode laser injection seeding was used to narrow the bandwidth of the broadband signal wavelengths. Injection seeding a nanosecond pulsed OPG in MgO:PPLN requires less than 1 mW [15]. The diode lasers each had a linewidth of approximately 1.5 GHz and were operated at a power of 4 mW and achieved sufficient seeding power to bandwidth convert each OPG. All diode lasers were vertically polarized with respect to the z-cut MgO:PPLN crystals. Three different diode lasers were used as injection seeders in the experiment. One laser was able to tune over a range of 1.47 μm to 1.54 μm. Another was able to tune from 1.52 μm to 1.57 μm. The last was able to tune from 1.38 μm to 1.47 μm. The multi-grating MgO:PPLN was maintained at a single desired frequency while the fan crystal was scanned over the full range

#229102 - $15.00 USD Received 4 Dec 2014; revised 18 Jan 2015; accepted 20 Jan 2015; published 5 Feb 2015

of each of the diode lasers. The injection seeded output bandwidth from each stage was 1.8 GHz which was comparable to each other.

The THz frequencies of interest were generated by mixing the output signal waves from the OPG in the DAST crystal. The output of each OPG stage was collimated and co-aligned. During the overlap process, the unconverted pump and idler wavelengths were removed from the system using frequency selective mirrors. The co-aligned beams were then passed through a half-wave plate in order to control the polarization angle of the combined linearly polarized beams.

To achieve optimal mixing in DAST, the combined narrowband OPG beams were focused in the crystal to a beam waist of 0.15 mm (1/e intensity diameters). The measured linewidth of both DFG pump beams is 1.8 GHz and was consistent across their individual tuning range. The emitted THz beam was then filtered from the unconverted signal beams. The filtering process was performed using either a high band pass germanium filter (HBP) or a low band pass (LBP) Germanium filter in combination with a stock germanium crystal (see Fig. 5). The generated THz beam was then collimated using an off-axis parabolic mirror and focused onto a pyro-electric detector. The pyro-electric detector was then synchronized with a chopper at a 7 Hz frequency using a lock-in amplifier. The chopper was placed directly after the output of MgO:PPLN multi-grating crystal. In addition, a power meter was used in the final examination of the system in place of the pyro-electric detector. In the final configuration three frequencies were selected and measured at peak output levels in which just one filter was used (HBP or LBP).

4. Results and discussion

The dual OPG source wavelengths were tuned to generate a frequency bandwidth between 1.5 THz and 27 THz. The DAST DFG THz wave was evaluated in three ways. Initially the generated THz waves were passed and filtered using a two filter process. Combinations of LBP Ge, HBP Ge, and stock germanium filters were used. The configuration served to reduce the unconverted signal power on the pyro-electric detector to a minimum. However, the method described also increased the overall absorption of the THz beam incident on the detector. The aforementioned method was implemented to partially sample a small range of the developed system. A comparison of the measured transmission was made with the known THz transmission spectrum in a range of 5 THz to 8 THz. The known transmission spectrum was generated at STP for a 3 m path length using HITRAN data [17]. The comparison between our experimental signal and HITRAN data is illustrated in Fig. 6.

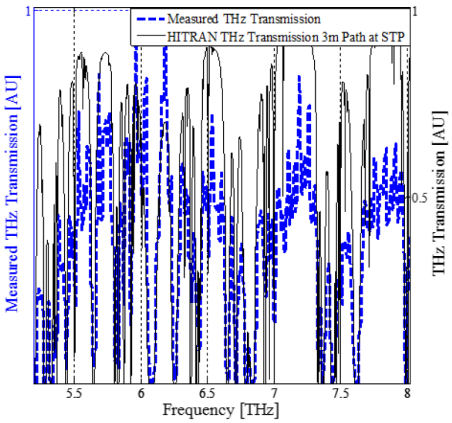

Fig. 6. Comparison of measured DFG system transmission with the known THz transmission spectrum in air for a 3 m path length at STP. No background corrections were made to the measured signal data.

#229102 - $15.00 USD Received 4 Dec 2014; revised 18 Jan 2015; accepted 20 Jan 2015; published 5 Feb 2015

In the mentioned measurement, the seed laser wavelengths were recorded. In the progression of the scan, the frequency was calculated and the measured THz signal was plotted as a function of frequency. When compared, a clear match was noted between the expected peaks and valleys in the transmission spectrum. Thus, the generated narrowband THz spectrum by means of the difference frequency process in DAST was validated. In addition, by measuring the narrowband water absorption we were able to estimate the linewidth of our system. The linewidth of the injection seeded OPG signal was approximately 1.8 GHz. Therefore, the expected linewidth of the generated THz beam should be on the same order. The measured features of the recorded spectrum is a convolution between the generated THz transmission beam and the water vapor line shape. The measured linewidth of our system was calculated to be 3.1 GHz that was constant across the tuning range of the system. The linewidth of the system was estimated from the resolved features of atmospheric absorption. The linewidth is calculated as a convolution between the known absorption features and the measured absorption features. Thus, such a system has a narrow bandwidth with a large dynamic range, which has distinct advantage over the conventional OPO systems with a linewidth of 5 GHz and limited to only 1-3 THz of tunability [18].

A full spectrum scan for our system was recorded and displayed in Fig. 7. Several OPG tuning frequency and temperature ranges were selected. To generate the desired wavelength range the MgO:PPLN multi-grating was held at a single output frequency while the fan crystal was swept across the IR spectrum to cover the desired tuning range. In addition, the spectral bandwidth remained at 3.1 GHz throughout the entire tuning wavelength range. The generated transmission scan is given in Fig. 7. The measured transmission spectra was generated using five overlapping spectral ranges.

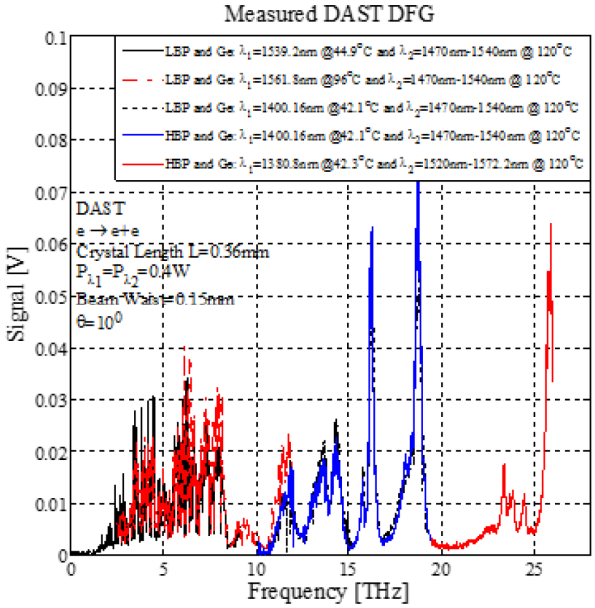

Fig. 7. Generated THz transmission spectrum from 1 THz to 27 THz. The data is presented without background correction and plotted using five different scans with partially overlapping scanning ranges and different filter combinations. The data was continuously recorded as the fan out MgO:PPLN crystal was tuned and scanned across the desired spectrum at a 3.1 GHz linewidth.

The variations of the power in the transmission spectrum observed in Fig. 7 are due to the phase miss-matching and absorption that is inherent to the DAST crystal. Multiple peaks and valleys occur in the spectrum, which can be attributed to the water vapor absorption due to the

#229102 - $15.00 USD Received 4 Dec 2014; revised 18 Jan 2015; accepted 20 Jan 2015; published 5 Feb 2015

propagation of THz in air. In order to evaluate the generated spectrum a comparison was made with the known atmospheric transmission model. Observed large signal dips such as those recorded at 20 THz are due to strong phonon absorption in DAST [5]. This strong phonon absorption could not be compensated for due to the intrinsic phase matching limitations of the DAST crystal which can be gauged by comparing the measured signal to the aforementioned model. Two separate criteria was used in the comparison. These criteria consisted of the polarization angle of the combined narrowband OPG beams, and the second parameter was to compare the power of the THz beam with the polarization maintained at a θ = 10° angle. A range of 3.8 THz to 12 THz was selected for the model comparison. Comparable power for both mixing wavelengths were selected to be 0.4 W incident on the DAST crystal.

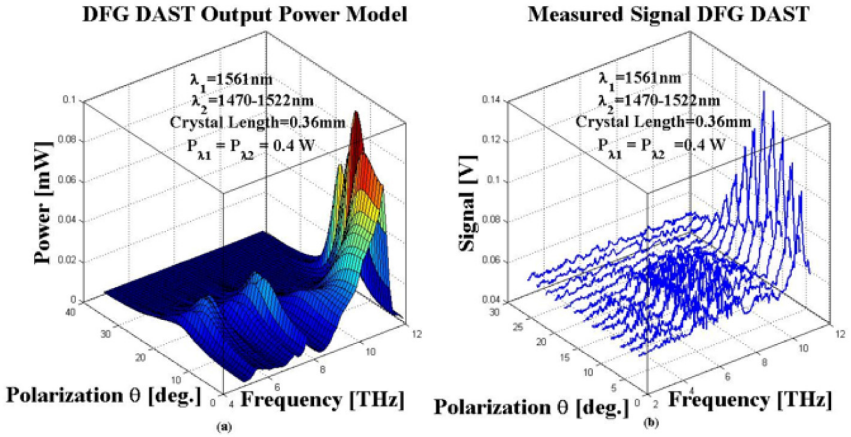

Fig. 8. Power output of DFG DAST. (a) Modeled DFG power as a function of polarization angle and frequency. (b) Measured DFG signal as a function of polarization angle and frequency. No background correction was performed and the data was recorded in increments of $\Delta\lambda$ = 0.15 nm.

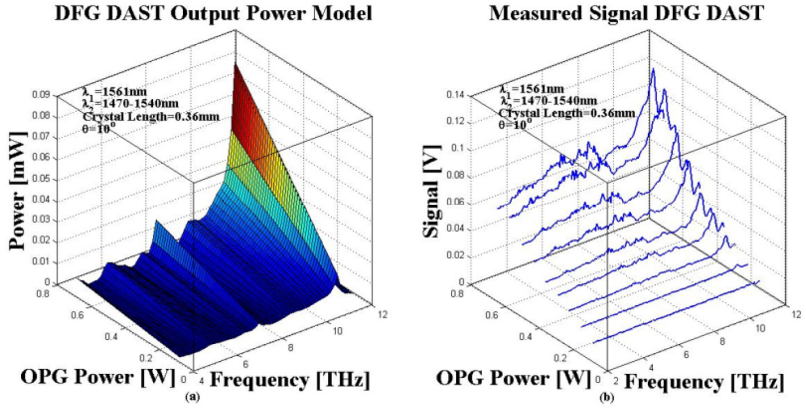

Fig. 9. Output power from DAST DFG. (a) Modeled output power as a function of OPG power and frequency. (b) Measured output power as a function of OPG power and frequency with no background corrections made and the data was taken at increments in $\Delta\lambda$ = 0.15 nm.

The measured signal and the modeled signal over the same frequency range are given in Fig. 8. The overall shape of the measured signal follows the same waveform structure as that of the modeled parameters. However, slight variations in the structure occur due to the sampling that was performed when the indices were measured for the known crystal structure.

#229102 - $15.00 USD Received 4 Dec 2014; revised 18 Jan 2015; accepted 20 Jan 2015; published 5 Feb 2015

The acquired indices and loss of the DAST in the THz domain were first taken with a tunable system at a larger bandwidth, with a different recording method, and with a different filtering technique [12]. Thus, minor differences in the generated THz spectrum and the modeled simulation were expected.

In the last evaluation of the generated THz signal, a power to signal strength trend comparison was performed with the combined narrowband OPG sources polarized at an angle of $\theta = 10°$. The selected frequency range of the signal was generated from 3.5 THz to 12 THz. In this comparison the dual OPG stages were equally reduced in power. The modeled power and the measured OPG power are given as a function of frequency in Fig. 9. The measured signal waveform structure closely follows the modeled power parameters. Minimal variations occur in the generated THz signal which are attributed to the germanium filters used and atmospheric absorption. When the power of the combined OPA fell below 0.3 W, the detector response used was negligible.

In addition, a high power scan was performed by filtering with a single filter only. In this measurement, four scans were overlapped to reach the full range of the system. The polarization angle of the combined beams was set at an angle of $\theta = 17°$. The power of the individual OPG injection seeded stages were set to 0.4 W each. The measured spectrum as a function of frequency is shown in Fig. 10.

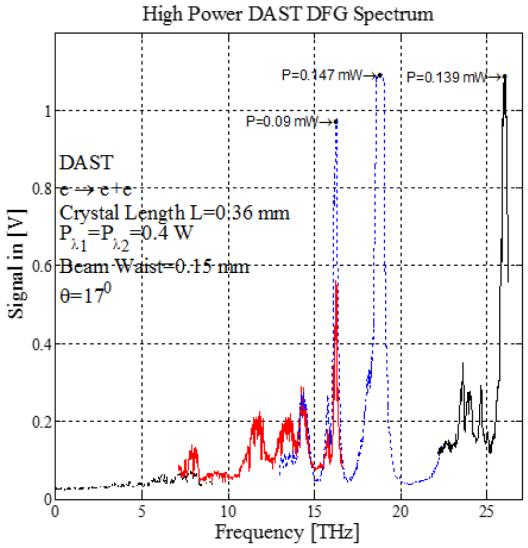

Fig. 10. Transmission spectrum using a single IR filter placed after the DAST crystal without background correction. The spectrum is a compilation of four different scans.

From the figure, it was noted that a power mismatch occurred. The expected features due to the water vapor absorption and phase mismatching were present. However, due to the selected polarization angle and reduced filtering, the higher frequencies were able to generate large signal gains when compared to the lower frequencies. The limitations can be attributed to the available filters for that specific range. The signal dips caused by phonon absorption could not be compensated for. The THz signal power was measured at three selected frequencies of 16.1 THz, 18.9 THz, and 26.5 THz. With the limitations noted, the system attained THz signal strengths at select frequencies exceeding 0.09 mW. For these frequencies optical conversion efficiency of 0.02% was achieved. Signal levels measured during the conversion process provide a large frequency tuning range from 1 to 28 THz and high power of 0.1 mW at select frequencies necessary for imaging applications. The dynamic range of our signal voltage measurements was about 30 dB.

#229102 - $15.00 USD Received 4 Dec 2014; revised 18 Jan 2015; accepted 20 Jan 2015; published 5 Feb 2015

5. Conclusion

To create a coherent THz-wave source with continuous narrowband frequency tunability based on the DFG DAST scheme, dual injection seeded OPG sources pumped with a 1.064 μm wavelength was developed. The tunability of the two OPG stages was successfully achieved by injection seeding two different MgO:PPLN crystals. When the tandem OPGs were combined as a source for the DFG method, a tunable narrowband THz source was demonstrated with DAST. We demonstrated a wide tunability with a high spectral resolution of 3.1 GHz for the generated THz spectrum between 1.5 THz and 27 THz. We measured the power and signal strength as a function of DFG frequency and as a function of combined OPG polarization angle. We demonstrated the dependence of the output THz wave power at a given frequency to the linear polarization angle of the combined mixing beams in the DAST. These measurements validate this method as suitable for many spectroscopic applications due to the resolution of the system and tunable power that can be produced. The simplicity and size of the THz source is an essential requirement for the development of future applications. When compared with available sources, the aforementioned nonlinear system presents distinct advantages in linewidth resolution, broad tunability, and ease of use.

Acknowledgments

The authors thank and acknowledge Doug Petkie and Jason Deibel of Wright State University for their assistance in THz detection. This work was partially supported by the U.S. Air Force Office of Scientific Research No. FA8650-09-D-5224.